Dynamic Zone Selection for Busbar Protection Using Graph Theory and Path Analysis

Rômulo. G. Bainy, Brian K. Johnson, and Armando Guzmán

***Abstract*—This paper presents a detailed description of a dynamic zone selection approach for busbar protection using path analysis and graph theory. The main benefit is that the dynamic zone selection logic equations for busbar protection applications are automatically obtained by an offline software-based tool. The method accounts for normal busbar-switching sequences, in-service transfer, bypassed current transformers, breaker substitution, paralleled busbars, and a check zone. The equations can be set up and executed in existing protective relays. The method was tested in a busbar arrangement for different switching scenarios and fault conditions, and the results have proven its effectiveness.**

***Keywords*—Power system protection, protective relaying, busbars, protection zone selection, graph theory, substation.**

NOMENCLATURE

BZB	Bus zone (BZ) connected to BZ (direct)
CBBZ	Circuit breaker (CB) connected to a BZ
CBPZ	Graph for the tripping zone
CTBZ	Current transformer (CT) connected to a BZ
CTPZ	Graph for the measuring zone
na, nb	Number of BZs and CBs
nc, nd	Number of CTs and Disconnect switches (DS)
PBZ	Paralleled BZs (direct and indirect)
PZS	Protection zone (PZ) supervision (enable PZ)
TF	Transfer-enable flag (disable check zone)
UBZb	Unbalanced BZ (CB/CT bypassed)
UBZt	Unbalanced BZ (in-service transfer)

I. INTRODUCTION

BUSBAR faults are rare in electric power systems; they account for only 6–7% of total faults [1]. These faults cause severe disturbances in the power system; they need to be cleared as fast as possible with minimum system disruption. A busbar fault typically leads to high current levels and can result in widespread blackouts because busbar disconnections cause large disruption of loads and generation [1] [2]. In large power substations, busbars are usually divided into protection bus zones [3]. Dynamic zone selection (DZS) plays a major role for busbar protection schemes by automatically assigning current transformers (CTs) to differential elements ensuring that relays operate according to Kirchhoff's current law [3], [4]. Additionally, the DZS determines which circuit breakers (CB) receive a trip command in case an internal busbar fault occurs.

One of the early developments regarding protection of complex busbar arrangements was presented in [5]. Their solution adopted two criteria to detect faults: directional comparison and differential current. However, in order to protect complex busbar arrangements, Haug and Forster's relay switched CT secondary current signals according to switching changes in the busbar arrangement. Using this system, potential hazardous catastrophes (e.g., open CT) can occur when the secondary circuit of a CT is switched off [6].

Previous efforts to improve the process of obtaining logic equations for dynamic zone selection were based on graph theory [7]–[10]. In a graphical representation, common branches (e.g., breaker, CT, breaker-CT, DS) are represented as edges and the rest of the components as vertices [7]–[9]. Three graph operations – edge contraction, ring sum, and vertex removal – are combined depending on the position and logical status of disconnect switches; therefore, the central unit relay has the duty to update the zone selection in real time whenever a switch is operated. Logic equations control protection zone supervision and the check zone, and they have the ability to handle faults occurring in the "end zone" (i.e., between the breaker and the associated CT). In [9], the authors considered a protection zone (PZ) as a protection area formed by at least one bus zone (BZ). Yet, a protection zone can include more than one bus zone if there is a solid connection between them. Whenever two or more bus zones are merged, a single protection zone arises, including all the adjacent connections. An important aspect to consider is that part of the logic equations have to be determined manually, which could be a challenging task. This paper presents a graphical approach to automatically generate all of the pertinent equations based on path analysis, removing the possibility of user error in entering the equations.

II. PATH ANALYSIS

The proposed method is called *Path Analysis* and uses graph theory to obtain the logic equations automatically. Advantages of the approach include the representation of measuring and tripping zones as graphs, which simplifies the expansion of existing busbar arrangements. Besides this advantage, no logic equations have to be determined by the end-user. The method is summarized in the following three steps:

- Transform the busbar arrangement into graphs
- Build the paths by using the graphs of the system
- Obtain the equations from the paths and store them

This work was supported by the Schweitzer Engineering Laboratories Inc.

R. G. Bainy and B. K. Johnson are with the University of Idaho, Moscow, ID 83844-1023 USA (e-mail: r.bainy@ieee.org and b.k.johnson@ieee.org).

A. Guzmán is with Schweitzer Engineering Laboratories, Inc., Pullman, WA 99163 USA (e-mail: armando_guzman@selinc.com).

Paper submitted to the International Conference on Power Systems Transients (IPST2021) in Belo Horizonte, Brazil, June 6–10, 2021.

A. Representing Busbar Arrangement Using Graphs

The busbar arrangement description consists of two graphs, which are called bay graph (G_1) and coupler graph (G_2). G_1 includes all busbars and elements of the bays, while G_2 contains devices associated with bus couplers and bus sectionalizers. The graphical representation considers three layers of information for the vertices and weighted edges, as shown in Fig. 1. The layers carry important information that maps the graphs to the original single-line diagram of the busbar arrangement. The first layer contains the unique number for each vertex, the second layer uses letters to identify the type of the device, and the last layer is the identification number of the device.

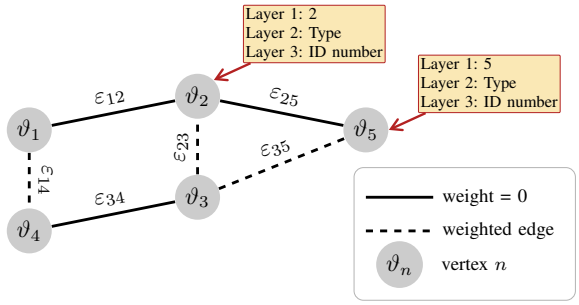

Fig. 1. Three layer and three–field graph representation

Table I summarizes the graphical representation of all elements of the busbar arrangement. The first column contains all components and the second one describes how each element is represented in terms of graphs. The third and forth columns show how layers 2 and 3 of the vertices are organized. Each component has a unique letter stored in Layer 2 and the number of the device from the electrical diagram is stored in Layer 3. Disconnect switches (DSs) and permanent electric connections (PECs) are represented as edges; the weight for a DS is equal to its number in the electrical diagram (e.g., the weight of the DS1 edge is one). Every DS has a different number, thus an exclusive weight, but PECs always have edge weights equal to zero. CTs are represented by two vertices to identify the polarity orientation; they are linked by an edge. The convergence node (CN) is an artificial vertex created whenever a CB vertex has more than two edges.

TABLE I
GRAPHICAL REPRESENTATION OF BUSBAR COMPONENTS

Component	Graphical Representation	Layer 2 Type	Layer 3 ID Number
Bus	Vertex	a	1 to na
Circuit Breaker	Vertex	b	1 to nb
Current Transformer	2 Vertices+edge	c and f	1 to nc
Network Element	Vertex	d	1 to nd
Convergence Node	Vertex	e	1 to ne
Disconnect Switches	Weighted edge	-	-
Permanent Connection	Edge	-	-

B. Building Paths

Graphs G_1 and G_2 are analyzed in terms of their subgraphs; they are created according to two criteria. The subgraph $H = (V_H, E_H)$ of graph $G = (V_G, E_G)$ is a distinct graph formed from a subset of vertices and edges of G; therefore, $V_H \in V_G$ and $E_H \in E_G$. Paths [11] are the type of subgraph of interest here because they are simple and can be defined as a tree in which no vertex has a degree greater than two. The number of edges in a path is always equal to $(n-1)$, where n is the number of vertices.

A graph can have a high number of paths; therefore, a considerable computational burden is required if all possible combinations are studied. To mitigate this issue, we define that only network elements and buses can be assigned as leaves of a path, that is, the leaf vertices must be type (Layer 2) a or d. This approach cuts down the number of possible paths to around 1–15% of all possible combinations [12]. The paths combined with the information of layers 2 and 3 contain important information regarding the station topology. The goal is to obtain the Boolean equations (BEs) by analyzing each path and store them in bus zone variables according to predefined criteria. The equations use status information from the auxiliary contacts of DSs and CBs.

C. Storing the Boolean Equations

The BEs obtained from the paths are stored in a set of variables, which can be represented as matrices. Their sizes depend on the number of CBs, CTs, and buses. The first subset of variables includes UBZb, BZB, CBBZ, and CTBZ. A bus zone (BZ) is an area surrounding a single bus and delimited by the injected currents measured by CTs. When it is impossible to measure one or more of the injected currents, the BZ is defined as an unbalanced bus zone and therefore defeated for differential protection purposes. Depending on the station layout and if the unmeasured current is part of a coupler or a bay, the BZ protection has to be either blocked or merged to another BZ. The variables UBZb and BZB are created to account for this condition. The variables CTBZ and CBBZ are used to define the measuring and tripping zones of the station. Fig. 2 shows the flowchart of how the BEs are stored. Each path is formed by leaves and branch vertices. The former are

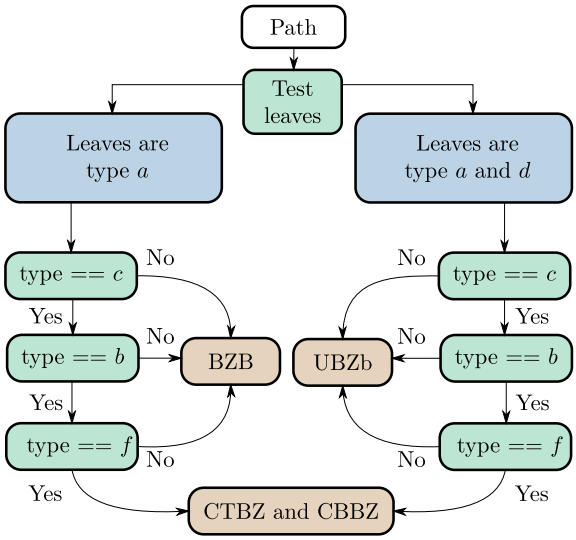

Fig. 2. Flowchart of how the BEs are stored into the variables

tested by the blue blocks in Fig. 2 and the latter are checked by the green ones. The vertex type (Layer 2) is used to choose the variable while the position inside the variable is defined by the ID of the vertex (Layer 3) [12].

PBZ, UBZt, and PZS are part of the second subset of dynamic zone selection variables; they are obtained by the combination of BZB and UBZb. The final graphs are named CTPZ and CBPZ. They account for the measuring and tripping zones, respectively, and are determined by combining the two subsets of variables. CBPZ is a graph that correlates CBs to PZs, while CTPZ is a directed graph that correlates CTs and PZs. A directed graph is a graph where the edges have a direction (e.g., arrow). We used this type of graph to represent the polarity of the CTs. The procedure is described in [12] and Fig. 3 shows a simplified flowchart of how the variables are combined. The zone selection is defined in terms of bus zones and protection zones. The protection zone is the result of merged and blocked bus zones according to the existence of paralleled buses or unbalanced bus zones. A station arrangement with na buses results in na protection zones and na bus zones. The protection zone and bus zone are identical (CTBZ = CTPZ and CBBZ = CBPZ) if no unbalanced bus zones or paralleled buses are present. This paper uses PBZ to account for paralleled buses by reconfiguring the protection zone with the lowest identification number to encompass all paralleled bus zones and by blocking their respective protection zone [13].

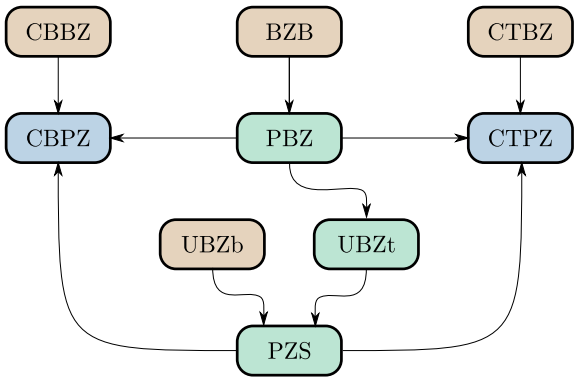

Fig. 3. Flowchart of how variables are combined

The method accounts for the creation of a single CZ by assigning all bay CTs to the CZ. However, the check zone becomes defeated whenever an inboard CT [3] is bypassed (i.e., when any element of UBZb is True). In such a scenario, its permissive flag must be replaced by a permanent permission or another type of supervision (e.g., undervoltage element), as suggested by IEEE Std 37.234 [3]. An additional variable called *transfer-enabled* (TF) stores all the switching combinations that result in an unbalanced check zone. In order to do so, the information stored at UBZb is combined as shown in (1). The check zone is always enabled for stations with only outboard CTs (TF = 0).

$$\mathrm{TF} = \sum_{i=1}^{na} \mathrm{UBZb}(i) \tag{1}$$

D. Representation of Measuring and Tripping Zones

The measuring zone (MZ) is represented as the directed multigraph $G_{MZ} = (V_{MZ}, E_{MZ})$ shown in Fig.4a [11]. Two sets of vertices are created: S_{ct} and S_{pz}. The former contains nc vertices (one for each CT). The latter consists of na vertices (one for each protection zone). The directed edges represent a connection between the sets S_{ct} and S_{pz}; the polarity of the current measured by the CT is indicated by the direction of the edge. Each edge ε is defined by three fields (s, t, and ℓ) as:

$$\varepsilon = (s, t, \ell) | \varepsilon \in E_{MZ} \tag{2}$$

where:

- s: source vertex (CT_i or $\mathrm{PZ}j$)
- t: target vertex (CT_i or $\mathrm{PZ}j$)
- ℓ: label that refer to the logic equation ($\mathrm{CT}_i\mathrm{PZ}_j$)

The tripping zone (TZ) is represented as the undirected graph $G_{TZ} = (V_{TZ}, E_{TZ})$ shown in Fig.4b [11]. This type of graph allows only one connection between vertices, and no orientation can be defined. The sets S_{cb} and the previously defined S_{pz} are utilized to build G_{TZ}. The set S_{cb} contains nb vertices (one for each breaker).

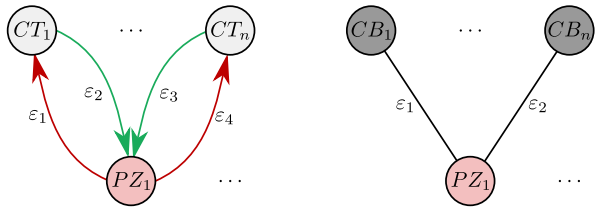

(a) CTPZ (G_{MZ}) (b) CBPZ (G_{TZ})

Fig. 4. Graph representation of CTPZ and CBPZ

E. Low-impedance differential protection scheme

Incidence of a vertex and edge is one of the properties of directed multigraphs that can be utilized on the implementation of a low-impedance busbar differential protection scheme. This property is exemplified in Fig. 4a, where edges ε_1 and ε_4 are incident *from* vertex PZ_1. Similarly, edges ε_2 and ε_3 are incident *to* vertex PZ_1. The graph G_{MZ} is updated in real-time; edges are included or removed according to the result of the logic equation stored in the field ℓ of the edge. Each vertex PZ_i of set S_{pz} is associated with two subsets of S_{ct} called S_t^i and S_f^i. The subset S_t^i contains all vertices of S_{ct} that are incident to vertex PZ_i. The subset S_f^i contains all vertices of S_{ct} that are incident from vertex PZ_i.

The operate $I_{PZ_i}^{op}$ and restrain $I_{PZ_i}^{res}$ currents are calculated for each protection zone PZ_i, as shown in (3) and (4), respectively.

$$I_{PZ_i}^{op} = \left| \sum^{j \in S_t^i} \overline{I_j} - \sum^{j \in S_f^i} \overline{I_j} \right| \tag{3}$$

$$I_{PZ_i}^{res} = \sum^{j \in S_{if}^i} |\overline{I_j}| \tag{4}$$

where i refers to each PZ, the set S^i_{tf} is the union of sets S^i_t and S^i_f; and $\overline{I_j}$ is the phasor of the current measured by the CT_j.

For each PZ, the operate current $I^{op}_{PZ_i}$ is compared with $I^{res}_{PZ_i}$ and a minimum threshold (I_{pickup}). The relay operates when $I^{op}_{PZ_i}$ exceeds I_{pickup} and a percentage of $I^{res}_{PZ_i}$, which is calculated using a *slope* value. Upon operation, the appropriate CBs have to be tripped. The concept of adjacency is utilized on G_{TZ} to generate the trip command T_i for each breaker CB_i. This property is exemplified in Fig. 4b, where vertex PZ_1 is adjacent to CB_1 and CB_n. Similarly to G_{MZ}, the graph G_{TZ} is updated in real-time; edges are included or removed according to the result of the logic equation stored in the field ℓ of the edge. Each vertex CB_i of set S_{cb} is associated with a subset of S_{pz} called S_i. The subset S_i contains all vertices of S_{pz} that are adjacent to vertex CB_i.

The trip command for each CB_i is calculated using (5).

$$T_i = \sum^{j \in S_i} 87\text{B}_j \tag{5}$$

where 87B_j indicates the operation of the 87B differential protection element of PZ_j.

III. Double-Bus and Bus-Coupler Arrangement

In this section, the dynamic zone selection variables are obtained using the *Path-Analysis* method for the double-bus and bus-coupler arrangement. Additionally, the graphs, paths, and BEs are discussed in detail. The double-bus and bus-coupler arrangement, shown in Fig. 5a, provides operational flexibility by enabling the connection of all bays to either bus, as well as only using one breaker per terminal. Nevertheless, under normal operation, its protection scheme follows a nearly straightforward single-bus configuration. However, dynamic zone selection or a busbar replica is required whenever a bay is transferred or a CB is under maintenance [3].

This station leads to the graphs G_1 and G_2 shown in Fig. 5b and Fig. 5c, respectively. For simplification, the graph G_1 considers only the busbars and Bay 1. The representation for the other bays is similar and is obtained by replacing the indices i and j according to Table II. Fig. 5d shows 5 out of the 17 paths for the double-bus and bus-coupler arrangement. The coupler graph, G_2, leads to path H_1. The bay graph, G_1, results in the four paths H_2–H_5. The other 12 paths refer to bays 2–4 and are equivalent to H_2–H_5. The paths shown in Fig. 5d result with the BEs listed in (6)–(10).

$$Eq_1 = S_{17} \cdot S_{18} \cdot \text{CB}_5 \tag{6}$$
$$Eq_2 = S_i \cdot S_{i+1} \tag{7}$$
$$Eq_3 = S_i \cdot S_{i+2} \cdot \text{CB}_j \tag{8}$$
$$Eq_4 = S_{i+1} \cdot S_{i+2} \cdot \text{CB}_j \tag{9}$$
$$Eq_5 = S_{i+3} \tag{10}$$

where equations Eq_6 to Eq_{17} are obtained by replacing the indices i and j with the values in each row of Table II.

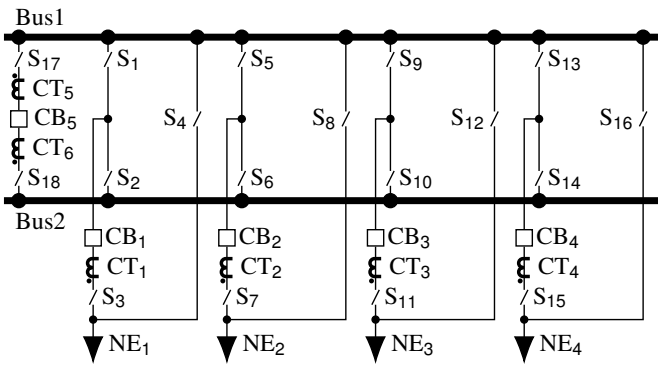

(a) Station: double-bus and bus-coupler arrangement

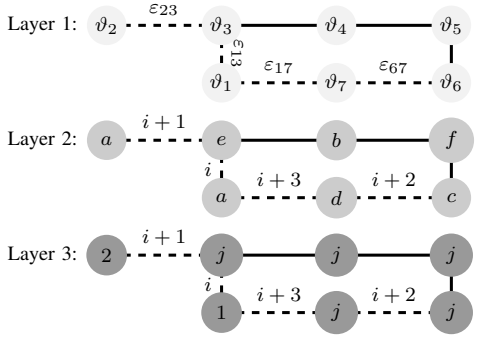

(b) G_1

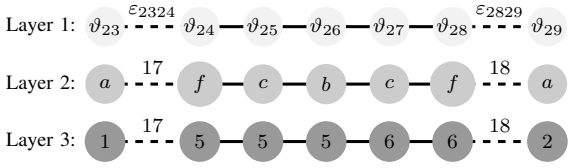

(c) G_2

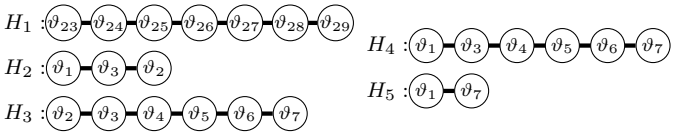

(d) Paths of the double-bus and bus-coupler arrangement (Bay 1)

Fig. 5. Graphs G_1 and G_2 for the double-bus and bus-coupler arrangement

The zone selection variables for this application are shown in (11)–(21).

$$\text{PBZ}_{12} = S_1 \cdot S_2 + S_5 \cdot S_6 + S_9 \cdot S_{10} + S_{13} \cdot S_{14} \tag{11}$$
$$\text{PZS}_1 = \textbf{NOT}(S_4 + S_8 + S_{12} + S_{16}) \tag{12}$$
$$\text{PZS}_2 = \textbf{NOT}(\text{PBZ}_{12}) \tag{13}$$
$$\text{CT}_5\text{PZ}_1 = 0 \tag{14}$$
$$\text{CT}_5\text{PZ}_2 = \text{PZS}_2 \cdot S_{17} \cdot S_{18} \cdot \text{CB}_5 \tag{15}$$
$$\text{CT}_6\text{PZ}_1 = \text{PZS}_2 \cdot \text{PZS}_1 \cdot S_{17} \cdot S_{18} \cdot \text{CB}_5 \tag{16}$$
$$\text{CT}_6\text{PZ}_2 = 0 \tag{17}$$
$$\text{CB}_1\text{PZ}_1 = \text{PZS}_1 \cdot \text{CB}_1 \cdot S_3 \cdot (S_1 + S_2 \cdot \text{PBZ}_{12}) \tag{18}$$
$$\text{CB}_1\text{PZ}_2 = \text{PZS}_2 \cdot \text{CB}_1 \cdot S_3 \cdot (S_2 + S_1 \cdot \text{PBZ}_{12}) \tag{19}$$
$$\text{CB}_5\text{PZ}_1 = \text{PZS}_2 \cdot \text{PZS}_1 \cdot S_{17} \cdot S_{18} \cdot \text{CB}_5 \tag{20}$$
$$\text{CB}_5\text{PZ}_2 = \text{PZS}_2 \cdot S_{17} \cdot S_{18} \cdot \text{CB}_5 \tag{21}$$

TABLE II
INDICES i AND j FOR BAYS 1–4 OF THE DOUBLE-BUS AND BUS-COUPLER ARRANGEMENT OF FIG. 5A

Index	Bay 1	Bay 2	Bay 3	Bay 4
i	1	5	9	13
j	1	2	3	4

The CBs and CTs of the bays are connected in series; therefore, the $\mathrm{CT}_m\mathrm{PZ}_n = \mathrm{CB}_m\mathrm{PZ}_n$, for $m = [1, 2, 3, 4]$ and $n = [1, 2]$. Generic equations are obtained for the other bay CTs, as listed in (22) and (23). The indices i and j assume the values from Table II. Additionally, identical equations to (22) and (23) also apply for $\mathrm{CB}_j\mathrm{PZ}_1$ and $\mathrm{CB}_j\mathrm{PZ}_2$, respectively.

$$\mathrm{CT}_j\mathrm{PZ}_1 = \mathrm{PZS}_1 \cdot \mathrm{CB}_j \cdot S_{i+2} \cdot (S_i + S_{i+1} \cdot \mathrm{PBZ}_{12}) \quad (22)$$

$$\mathrm{CT}_j\mathrm{PZ}_2 = \mathrm{PZS}_2 \cdot \mathrm{CB}_j \cdot S_{i+2} \cdot (S_{i+1} + S_i \cdot \mathrm{PBZ}_{12}) \quad (23)$$

where i and j assume the values from Table II.

The check zone is obtained using (24):

$$\mathrm{CT}_j\mathrm{CZ} = \begin{cases} 1 & j \leq 4 \\ 0 & j \geq 5 \end{cases} \Bigg| \, 0 < j \leq 6 \quad (24)$$

This station contains inboard CTs (i.e., from CT_1 to CT_4); therefore, the check zone gets unbalanced if any of the inboard CTs are bypassed. This condition is accounted for by TF:

$$\mathrm{TF} = S_4 + S_8 + S_{12} + S_{16} \quad (25)$$

IV. DYNAMIC ZONE SELECTION STUDY

In this section, the double-bus and bus-coupler arrangement shown in Fig. 5a is simulated in different switching scenarios and fault conditions. The goal is to highlight the effectiveness of the dynamic zone selection equations determined in the previous section. In order to do so, the station was simulated using a real-time digital simulator. The runtime interface utilized in the real-time simulator used for this project is shown in Fig. 6. The DZS equations were implemented using a custom component created with the module CBuilder and a commercially available relay. The network elements (NE) are represented as Thevenin equivalents and the data are listed in the Appendix.

Four cases were studied with different switching scenarios and fault locations. The zone selection logic is implemented using a custom component created with the CBuilder. Additionally, the logic equations were combined in a commercially available relay [14] using Relay Word Bits (RWBs). The main RWBs configured for this application regarding zone selection are BZpBZmV, IqqBZn, ZnS, and CZ1S. They are programmed according to (26)–(29).

$$\mathrm{BZ}p\mathrm{BZ}m\mathrm{V} = \mathrm{PBZ}_{pm} \quad (26)$$

$$\mathrm{I}qq\mathrm{BZ}n = \mathrm{CT}_{qq}\mathrm{BZ}_n \cdot \textbf{NOT}\ \mathrm{UBZb}_n \quad (27)$$

$$\mathrm{Z}n\mathrm{S} = \textbf{NOT}(\mathrm{UBZb}_n \cdot \mathrm{UBZt}_n) \quad (28)$$

$$\mathrm{CZ1S} = \textbf{NOT}\ \mathrm{TF} \quad (29)$$

The four cases are summarized as: normal operation (Case 1), buses directly connected or in parallel (Case 2), CB_1 bypassed (Case 3), and fault at the overlapped area of the PZs (Case 4). These scenarios are represented by maneuvering the DSs and CBs. Initially, all DSs and CBs are closed except DSs 2, 4, 5, 8, 10, 12, 13, and 16, as shown in Fig. 7a. NE_1 and NE_3 are connected to Bus 1, while NE_2 and NE_4 are connected to Bus 2. The measuring and tripping zones are represented by the graph in Fig. 7b. PZ_1 and PZ_2 are represented by the colors pink and cyan, respectively.

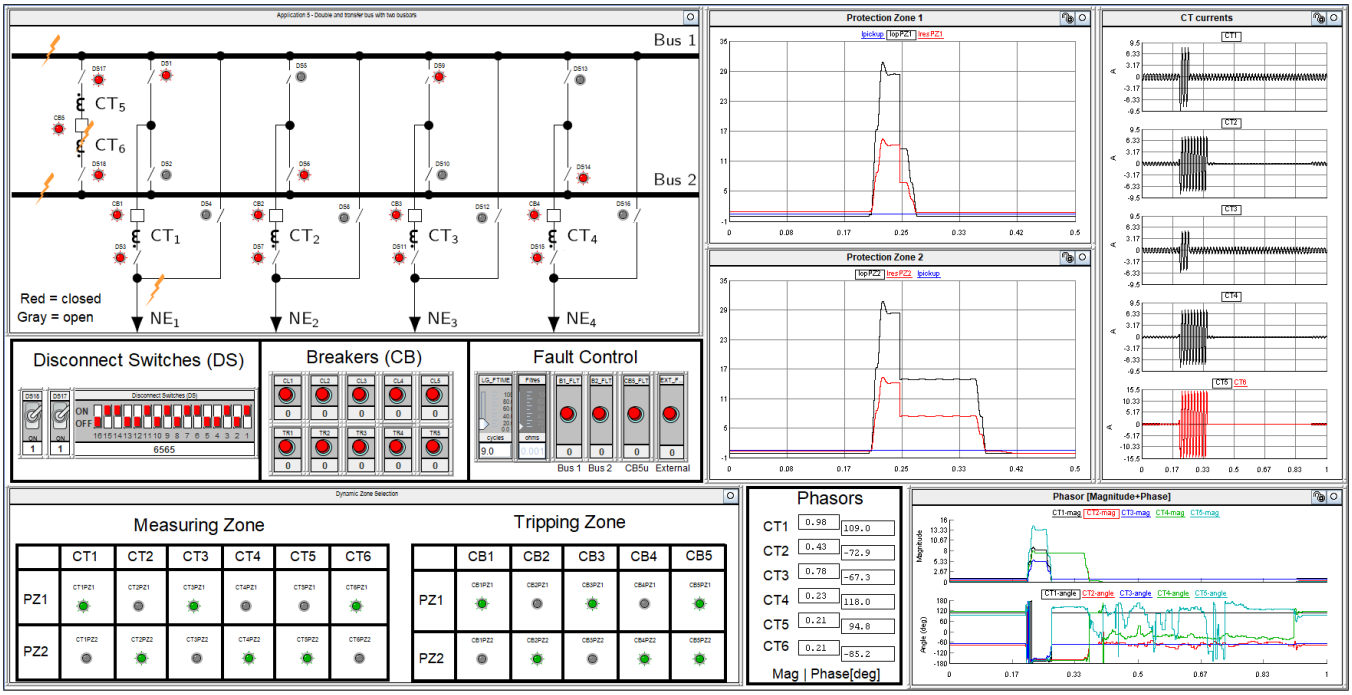

Fig. 6. Runtime interface simulated in the real time simulation environment

The relay includes a sequential events recorder (SER), which monitors user-defined elements, such as RWBs, inputs, and outputs. An SER report lists time-tagged events logged whenever a monitored element changes its state. To represent the zone selection, the SER monitors RWBs (BZpBZmV, IqqBZn, ZnS, and CZ1S). Additionally, the ZONE command available in the relay was used to list the currents assigned to each protection zone.

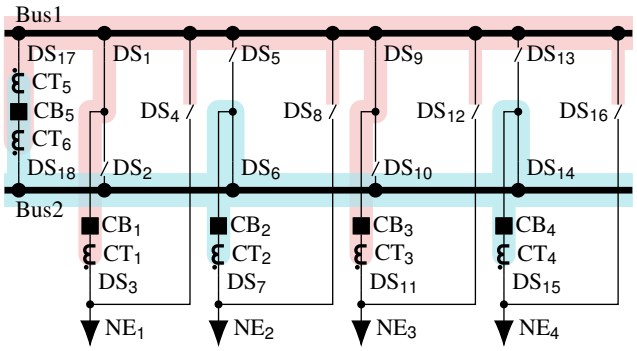

(a) Normal operation

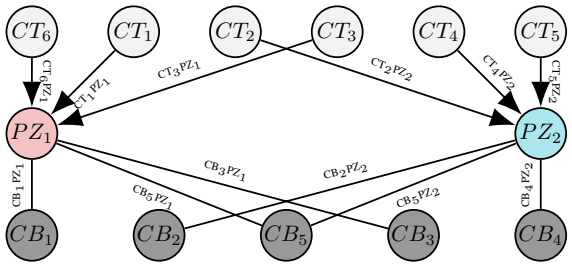

(b) Measuring and tripping zones

Fig. 7. Measuring and tripping zones under normal operation

A. Case 1: Normal Operation and fault at Bus 1

Case 1 studies the station under normal operation, the ZONE command reported by the relay is shown in Fig. 8. Protection zone 1 contains only the Bus Zone 1 (BZ1). The CTs 1, 2, and 6 (labeled as I01, I02, I06, respectively) are part of BZ1. Similarly, Protection Zone 2 contains only BZ2. The CTs 3, 4, and 5 (labeled in the relay as I03, I04, I05, respectively) are part of BZ2.

```
=>ZONE
Terminals in Bus Zone 1:                    I01, I03, I06
Bus Zones in Protection Zone 1:             BZ1
Terminals in Bus Zone 2:                    I02, I04, I05
Bus Zones in Protection Zone 2:             BZ2
```

Fig. 8. ZONE command for Case 1

In this case, PZ_1 and PZ_2 are balanced; therefore, they only operate if an internal fault occurs. Upon inception of a fault at Bus 1 with fault resistance of 10Ω, the operate and restrain currents increase. As Fig. 9 shows, the differential element of PZ_1 operates ($slope = 0.5$ and $I_{pickup} = 1.0\ pu$) and isolates the fault by tripping CB_1, CB_3, and CB_5. The fault is external to PZ_2; therefore, the relay does not detect a fault in PZ_2.

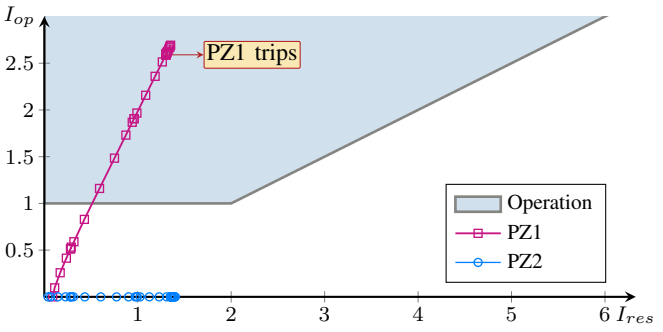

Fig. 9. Internal fault at Bus 1 seen by the differential elements of PZ_1 and PZ_2

B. Case 2: Paralleled buses

Case 2 is the switching scenario where DSs 1 and 2 are closed simultaneously, thus causing buses 1 and 2 to be directly connected. The current flowing through these switches cannot be measured; therefore, the buses have to be protected as one PZ. The zone selection algorithm adjusts the measuring and tripping zones as shown by the station and graphs shown in Fig. 10a and Fig. 10b, respectively. PZ_1 encompasses both buses, while PZ_2 is inactive.

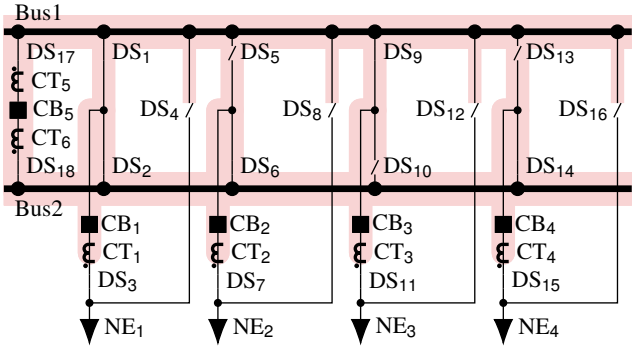

(a) Paralleled buses

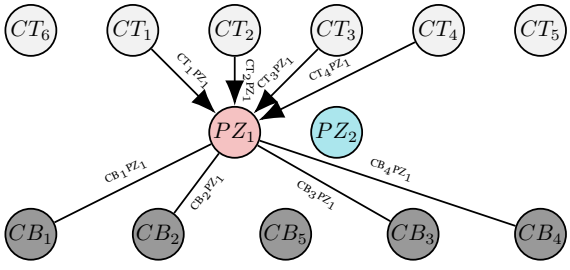

(b) Measuring and tripping zones

```
=>SER
#    DATE          TIME              ELEMENT  STATE
4    09/10/2020    21:57:12.4416     I05BZ2V  Deasserted
3    09/10/2020    21:57:12.4416     I06BZ1V  Deasserted
2    09/10/2020    21:57:12.4416     BZ1BZ2V  ASSERTED
1    09/10/2020    21:57:12.4416     Z2S      BLOCKED
=>ZONE
Terminals in Bus Zone 1:                    I01, I02, I03, I04
Bus Zones in Protection Zone 1:             BZ1, BZ2
Protection Zone 2 is Inactive
```

(c) SER and ZONE command results for Case 2

Fig. 10. Case 2: Paralleled buses

The SER and ZONE commands of the relay are shown in Fig. 10c. PZ_1 now encompasses both BZs. The SER command shows that I06BZ1V was deasserted, which means that the CT_6 was removed from PZ_1 to avoid overrestrain operation of Protection Element 1. The element BZ1BZ2V was asserted; Protection Zone 1 now encompasses BZ1 and BZ2, as reported by the ZONE command.

C. Case 3: CB_1 bypassed

Case 3 consists of the substitution of CB_1 by CB_5. Such a condition occurs when, for example, a breaker of a bay is under maintenance. The only difference between this scenario and Case 1 is that DSs 4 and 10 are closed and DS_9 is open. Under this condition, Bus 1 cannot be protected by the differential element because the current (I_{bp}) flowing at DS_4 is not measured by any of the available CTs. As a result, PZ_1 is inactive and PZ_2 remains active, encompassing all CTs and CBs connected to Bus 2, as shown in Fig. 11b. The SER of the relay is shown in Fig. 11c. Z1S blocks BZ1 and PZ1; CT_1 and CT_6 are removed from the BZ1 by deasserting elements I01BZ1V and I06BZ1V, respectively. The ZONE command report is also shown in Fig. 11c. PZ_1 is inactive; therefore, no CT or CB is assigned to it. On the other hand, PZ_2 remains the same and encompasses only BZ_2.

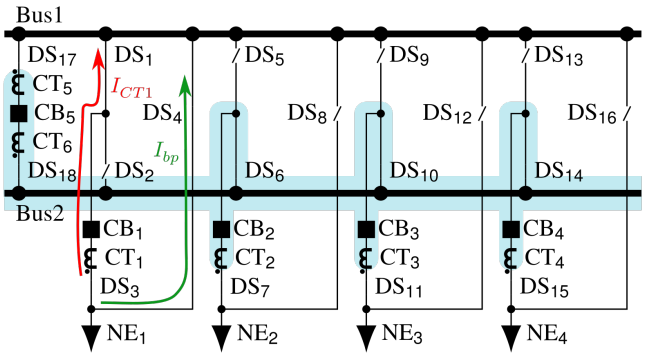

(a) CB_1 is bypassed

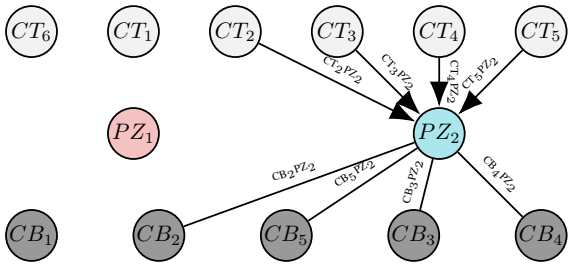

(b) Measuring and tripping zones

```
=>SER
#        DATE          TIME            ELEMENT  STATE
3        09/10/2020    22:08:12.7728   I01BZ1V  Deasserted
2        09/10/2020    22:08:12.7728   I06BZ1V  Deasserted
1        09/10/2020    22:08:12.7728   Z1S      BLOCKED
=>ZONE
Protection Zone 1 is Inactive
Terminals in Bus Zone 2:                I02, I03, I04, I05
Bus Zones in Protection Zone 2:         BZ2
```

(c) SER and ZONE command results for Case 3

Fig. 11. Case 3: CB_1 is bypassed

D. Case 4: Fault between CB_5 and CT_6

Lastly, Case 4 studies a sequence of events that starts with the station under normal operation, as in Fig. 7a. Next, a phase-to-ground fault occurs between CB_5 and CT_6 as shown in Fig 12a. Protection zones 1 and 2 detect an internal fault, because the fault occurred at the overlapped area of the PZs. However, to isolate the fault only PZ_2 has to be tripped. In this situation two approaches are commonly used 1) Trip both protection zones, 2) Trip the tie-breaker, remove the CTs surrounding the tie-breaker, and finally trip the proper protection zone [3]. The first approach is faster because no extra timers are added to the regular tripping logic. However, the second approach is more selective because PZ_1 remains active while PZ_2 is tripped to isolate the fault. The second approach was implemented here; therefore, after the CB_5 is tripped, CT_5 and CT_6 are removed by the dynamic zone selection algorithm. Fig. 12b shows the expansion of the protection zones which are now limited by the terminals of CB_5. The measuring and tripping zones are rearranged to the graphs shown in Fig. 12c. The dynamic zone selection affects the operational plane; at first, the differential element of both PZs lay in the operation area. However, the differential element PZ_1 returns to the restrain area after CB_5 is tripped, as plotted in Fig. 12d. PZ_2 isolates the fault by tripping CBs 2 and 3.

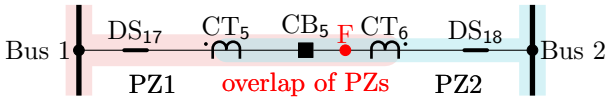

(a) PZ1 and PZ2 detect an internal fault

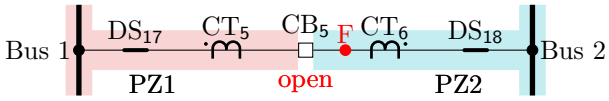

(b) Trip the tie-breaker (CB_5) before the PZs

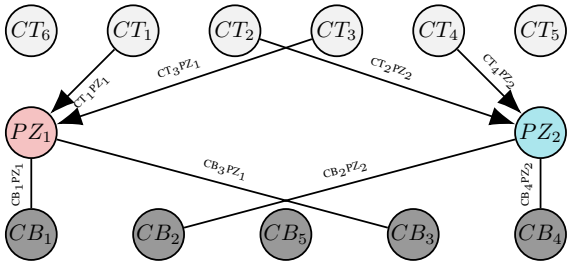

(c) Measuring and tripping zones after CB_5 opens

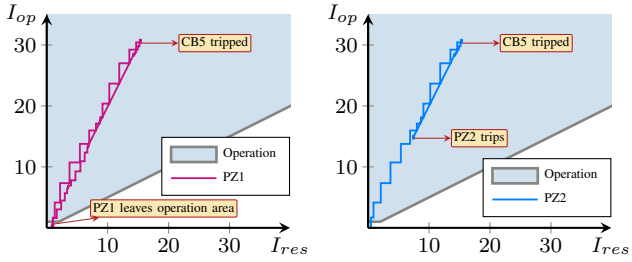

(d) Fault between CT_6 and CB_5 seen by the PZ_1 and PZ_2

Fig. 12. Case 4: Fault at the overlay region of PZs 1 and 2

V. Conclusion

This paper expands and proposes the *Path-Analysis* method in detail by using a double-bus and bus-coupler arrangement. The method obtains logic equations and two graphs to achieve proper dynamic zone selection. The measuring and tripping zones are represented as a directed multigraph and a undirected graph, respectively. This representation enables simpler implementation dynamic zone selection and expansion of the busbar arrangement. The presented results confirm sufficient versatility of the method for different switching scenarios and fault conditions. One of the benefits of this method is the ability to automatically obtain the zone selection equations without requiring the engineer or relay technician to enter logic equations as inputs. Additionally, the method can be implemented in software using only the single-line diagram of the station; therefore, reducing errors and time required to set the relay. Furthermore, the method follows guidelines for busbar protection presented in IEEE Std-C37.234 and can be used for different busbar arrangements.

VI. Appendix

The busbar arrangement simulated in this paper contains four network elements that are represented as voltage sources and series impedances. Table III presents the values for all the parameters. The per–unit values were calculated using voltage and power bases of 230 kV and 150 MVA, respectively. The voltages of all sources are set to 1 pu.

TABLE III
Data of the Power System Simulated

NE	$R_1[\Omega]$	L_1[mH]	Θ	NE	$R_1[\Omega]$	L_1[mH]	Θ
1	12.05	49.8	0°	3	18.70	77.3	-15°
2	13.39	55.3	-10°	4	15.01	51.4	-5°

VII. Acknowledgment

The authors acknowledge the contributions of N. Fischer for his suggestions throughout this work.

References

[1] C. Martin *et al.*, "Bus Protection Considerations for Various Bus Types," in *69th Annual Georgia Tech Protective Relaying Conference*, Atlanta, Georgia, 2015, pp. 1–9.
[2] P. Kundur, *Power System Stability and Control*. McGraw-Hill, 2006.
[3] *IEEE Guide for Protective Relay Applications to Power System Buses*, IEEE C37.234™-2009 Std., Sep. 2009.
[4] Cigre WG B5.16, "Modern Techniques for Protecting Busbars in HV Networks," Cigre, Tech. Rep., Oct. 2010.
[5] H. Haug and M. Forster, "Electronic Bus Zone Protection," in *International Conf. on Large High Tension Systems*. Paris: CIGRÉ, 1968.
[6] J. L. Blackburn and T. J. Domin, *Protective relaying: principles and applications*, 4th ed. CRC Press, 2014.
[7] B. L. Qin, A. Guzmán, and E. O. Schweitzer, III, "A new method for protection zone selection in microprocessor-based bus relays," *IEEE Transactions on Power Delivery*, vol. 15, no. 3, pp. 876–887, Jul. 2000.
[8] B. L. Qin and A. Guzmán, "System for protection zone selection in microprocessor-based relays in an electric power system," U.S. Patent 6,411,865 B1, Jun. 25, 2002.
[9] A. Guzmán and C. Labuschagne, "Reliable busbar protection with advanced zone selection," *IEEE Transactions on Power Delivery*, vol. 20, no. 2, pp. 625–629, Apr. 2005.
[10] S. Sheng, L. Jianhua, X. Hui, and J. Dongjun, "Expert System for Wide Area Protection Zone Selection," in *Transm. and Distrib. Conf.: Asia and Pacific*. China: IEEE, 2005.
[11] W. K. Chen, *Graph Theory and Its Engineering Applications*. World Scientific, 1997.
[12] R. G. Bainy, K. M. Silva, S. Lotfifard, A. Guzmán, and B. K. Johnson, "Dynamic zone selection for busbar protection based on graph theory and boolean algebra," *IEEE Transactions on Power Delivery*, vol. 35, no. 4, pp. 1769–1778, 2020.
[13] *IEEE Guide for Breaker Failure Protection of Power Circuit Breakers*, IEEE C37.119™-2016 Std., May 2016.
[14] *SEL-487B-1 Bus Differential and Breaker Failure Relay Instruction Manual*, Schweitzer Engineering Laboratories, Inc., 2018.

Rômulo G. Bainy received the Ph.D. degree from the University of Brasília (UnB), Brazil in 2019. He was a visiting scholar in Washington State University, Pullman, USA, in 2018. His research interests are in power system protection, fault location, electromagnetic transients, renewable energy, and CCVTs. He is a reviewer for IEEE Transactions journals and IEEE conferences.

Dr. Bainy is a Postdoctoral Fellow in the University of Idaho, Moscow, USA.

Brian K. Johnson received his doctoral degree in EE at the University of Wisconsin-Madison in 1992. He is the Schweitzer Engineering Laboratories Endowed Chair in Power Engineering and a Professor in the University of Idaho ECE Department. His interests include power systems applications of power electronics, power system protection, and power system transients.

Dr. Johnson is a registered professional engineer in the State of Idaho.

Armando Guzmán received his BSEE with honors from Guadalajara Autonomous University (UAG), Mexico. He received a diploma in fiber-optics engineering from Monterrey Institute of Technology and Advanced Studies (ITESM), Mexico, and his masters of science and Ph.D. in electrical engineering and masters in computer engineering from the University of Idaho, USA. He served as regional supervisor of the Protection Department in the Western Transmission Region of the Federal Electricity Commission (the electrical utility company of Mexico) in Guadalajara, Mexico for 13 years. He lectured at UAG and the University of Idaho in power system protection and power system stability. Since 1993 he has been with Schweitzer Engineering Laboratories, Inc. in Pullman, WA, where he is a distinguished engineer. He holds numerous patents in power system protection and metering.